Talanta 81 (2010) 1409–1412

Contents lists available at ScienceDirect

Talanta

journal homepage: www.elsevier.com/locate/talanta

Sequential injections as an alternative to gradient exploitation for implementing differential kinetic analysis in a flow injection system

Paula R. Fortes[a], Mario A. Feres[a], Elias A.G. Zagatto[a,*], José L.F.C. Lima[b]

[a] Centre for Nuclear Energy in Agriculture, University of São Paulo, P.O. Box 96, Piracicaba 13400-970, Brazil
[b] REQUIMTE, Faculdade de Farmácia da Universidade do Porto, Rua Aníbal Cunha 86, Porto 4099-030, Portugal

ARTICLE INFO

Article history:
Received 3 December 2009
Received in revised form 11 February 2010
Accepted 15 February 2010
Available online 24 February 2010

Keywords:
Flow injection analysis
Differential kinetics
Partial least squares
Catalytic methods
Spectrophotometry
Alloy analyses

ABSTRACT

A novel flow-based strategy for implementing simultaneous determinations of different chemical species reacting with the same reagent(s) at different rates is proposed and applied to the spectrophotometric catalytic determination of iron and vanadium in Fe–V alloys. The method relies on the influence of Fe(II) and V(IV) on the rate of the iodide oxidation by Cr(VI) under acidic conditions; the Jones reducing agent is then needed. Three different plugs of the sample are sequentially inserted into an acidic KI reagent carrier stream, and a confluent Cr(VI) solution is added downstream. Overlap between the inserted plugs leads to a complex sample zone with several regions of maximal and minimal absorbance values. Measurements performed on these regions reveal the different degrees of reaction development and tend to be more precise. Data are treated by multivariate calibration involving the PLS algorithm. The proposed system is very simple and rugged. Two latent variables carried out *ca* 95% of the analytical information and the results are in agreement with ICP-OES.

1. Introduction

Since the landmark contribution by Dahl et al. demonstrating the feasibility of implementing differential kinetics in flow analysis [1], several approaches for simultaneous determinations have been proposed. The original procedure aimed at magnesium and strontium determinations and involved two spectrophotometers: the related flow-through cuvettes were placed at two different sites of the analytical path. In this way, two peaks were registered per sample, each one corresponding to a given mean available time for reaction development. As the sample and reagent volumetric fractions were not constant from one monitoring site to another, the procedure can be regarded as a pseudo-differential kinetic analysis. The approach was further applied to the determination of calcium and magnesium exploiting the cryptand (2.2.1) complexes of Ca^{2+} and Mg^{2+} in the presence of Na^{+} as scavenger [2]. By exploiting the better selectivity attained with the cryptand (2.2.2) complexes of Ca^{2+}, Mg^{2+} and Sr^{2+}, other analogous analytical procedures were proposed for the simultaneous determinations of calcium plus strontium or magnesium plus strontium [3]. However, these pioneer contributions required two spectrophotometers, being then less suitable for large-scale analysis.

The drawback was circumvented by taking advantage of stream splitting/merging [4]. The flowing sample was split and the formed zones were directed towards two parallel reactors with different characteristics; the outlet streams merged together immediately before detection. In this way, different sample-to-reagent volumetric ratios, sample dispersions and mean available times for reaction development corresponded to each sample. Only one detector was needed. The feasibility of the approach was demonstrated in the spectrophotometric determinations of cobalt and nickel, the catalytic fluorimetric determinations of manganese and iron, and the fluorimetric determination of pyridoxal and pyridoxal-5-phosphate [5,6]. It was also applied to fluorimetric determinations of silicate and phosphate in natural waters based on the different rates of molybdenum blue formation [7], and to the determinations of furfural and vanillin in synthetic samples based on the different reaction rates of these compounds with *p*-aminophenol [8]. More recently, uncertainties in the sample splitting were minimized by using computer-assisted splitting, and this was accomplished by adding a three-way valve in the split point [9].

The need for two spectrophotometers can be also avoided by using a homemade device including two flow cells trespassed by the incident radiation beam of the spectrophotometer [10,11]. The flowing sample flew successively through the first flow cell and a delay coil, reaching thereafter the second flow cell where it was monitored again under conditions of higher dispersion and longer mean resident time. Multi-site detection [12] can be also exploited to permit a single detection unit to monitor at two different

* Corresponding author. Tel.: +55 19 34294650; fax: +55 19 34294610.
E-mail address: ezagatto@cena.usp.br (E.A.G. Zagatto).

0039-9140/$ – see front matter © 2010 Elsevier B.V. All rights reserved.
doi:10.1016/j.talanta.2010.02.044

manifold sites. The usefulness of the approach was demonstrated in the determination of copper and zinc in plant digests using Br-PADAP as the colour-forming reagent [13].

Two analytes reacting with a common reagent at different rates can be also determined by injecting the sample and stopping the sample zone at the detector. In this way, two absorbance values can be obtained. The strategy was applied to the spectrophotometric determinations of mercury plus zinc [14] and copper plus zinc [15] in synthetic water samples as well as of chorpyrifos and carbaryl in pharmaceutical formulations [16]. Dual sample injection into two different confluent carrier streams [8,10] has also been exploited. Another possibility is to take advantage of commutation in order to provide reactor replacement. The sample was injected twice, and to each injection a different reactor was inserted into the analytical path, thus providing two conditions for methodological implementation. The innovation was demonstrated in the spectrophotometric determination of cobalt and nickel in tool steels [17].

Use of stream splitting/merging, dual sample injection or two flow-through cuvettes at different manifold sites were critically compared [18]. However, the related procedures rely on two measurements performed under different sample handling conditions that allow solving a simple equation system.

A more robust data treatment involving a number of measurements per sample can be attained by exploiting the concentration gradients established along the sample zone [19]. Each slice of the recorded peak refers to a fluid element characterized by a given mean residence time, a given analyte concentration and specific conditions for reaction development [20].

Better analytical information can be obtained when a large sample volume is injected into the reagent carrier stream, as the resulting concentration gradients become more pronounced. The information related to these regions can be used for building-up and calibrating multi-parametric models as it contains time-dependent information [21]. When differential kinetics is aimed, better discrimination is attained, as each slice – thus each measurement – refers to a different degree of reaction development. It is then possible to quantify two or more analytes which reacts with the same reagent(s) at different rates [22,23].

Lower measurement precision is however associated to the sample regions associated to the rise and fall of the recorded peak. In this way, these regions should not be considered for building-up the mathematical models. In order to attain several reproducible measurements, successive sequential sample injections into the reagent carrier stream can be used. Partial overlap of the sample zones results in a complex zone which presents several regions of maximal and minimal concentrations, and better measurement precision is inherent to these regions [24].

The aim of this work was to design a flow system able to provide the kinetic–spectrophotometric information needed for differential kinetic analysis. This work is a refinement of earlier study [22], and the main difference consists in taking into account the measurements performed on the maximum and minimum values of the recorded peak and not those inherent in the concentration gradients. The strategy intends to improve the analytical precision, as the time delay between instants of sample injection and measurement of specific slices constituted itself in the main source of results dispersion in the earlier application. Moreover, the standard solutions were prepared to cover narrower concentration ranges in order to improve accuracy.

The present study was carried out in a classical flow injection system, a less versatile system when compared with the multipumping flow system [25] used in the original procedure. As the innovation holds for any flow-based unsegmented flow analyzer, and considering that flow injection analysis is worldwide utilised by the scientific community, one expects then a wider acceptance of the proposed innovation.

2. Experimental

2.1. Solutions

The alloy samples were washed with 0.01 mol L^{-1} HNO_3, dried and drilled. One hundred milligrams of the resulting fillings was weighed and placed into 250-mL Erlenmeyer flasks, to which *ca* 10 mL of *aqua regia* (3:1::HCl:HNO_3, v/v) were added. The flasks were placed on a hot plate until complete dissolution. After cooling to room temperature, 5.0 mL of 70% (v/v) $HClO_4$ were added and the flasks were heated until evolution of white fumes. The volumes of the residual solutions were then made up to 100 mL with water [26]. Before analyses, the sample solutions underwent a 50-fold manual dilution with 0.01 mol L^{-1} HCl.

The stock standard solutions (1000 mg L^{-1}) were based on $FeCl_3{\cdot}6H_2O$ and V_2O_5. They were prepared by dissolving the required amounts in 10 mL of 7.0 mol L^{-1} HNO_3 and diluting to 1000 mL with water. The working standard solutions were 8.0–10.0 mg L^{-1} Fe plus 6.0–8.0 mg L^{-1} V, also 0.01 mol L^{-1} HCl. Immediately before analyses, the diluted samples and the standard solutions were passed through a Jones reductor mini-column [27] for quantitative reduction of Fe(III) and V(V) to Fe(II) and V(IV).

The R_1 reagent was a daily prepared 1.0×10^{-1} mol L^{-1} KI solution and the R_2 reagent was a 1.0×10^{-3} mol L^{-1} Cr (as $K_2Cr_2O_7$) solution, both prepared in 0.01 mol L^{-1} HCl [27].

2.2. Apparatus

A FIAlab–3000 flow analyser including a model USB 2000 UV–vis Ocean Optics spectrophotometer and an acrylic Z-shaped flow cell (inner volume = 10 μL, optical path = 10 mm) was used. A model IPC 8R Ismatec peristaltic pump was used as fluid propeller and a MTV-3-N1/4UKG three-way solenoid valve (Takasago Electric Inc., Nagoya, Japan) as a fluid directing device. They were operated through a power driver based on the PCL-711 Advantech interface card and the Quick Basic 5.0 software. Data treatment was performed with the PLS Toolbox (Eigenvector Technologies, Inc) included in the MATLAB version 6.5c (The Math. Works, Inc.) computer package.

The manifold was build-up with polyethylene tubing (i.d. = 0.8 mm) of the non-collapsible wall type. Acrylic connectors and accessories were also used.

2.3. Flow diagram

The flow injection system is shown in Fig. 1. The timing course of the V valve determined the sample injected volumes and the time intervals between injections [28]. Three different sample plugs were inserted sequentially into the R_1 reagent carrier stream, leading to formation of a complex overlapped sample zone. To this end, the valve was turned ON for three times, inserting the S_1, S_2 and S_3 sample plugs and defining the Δt_1 and Δt_2 time intervals between them (Table 1). The sample zone underwent continuous dispersion while being transported through the analytical path, and concentration gradients were formed along it.

Thereafter, R_1 and R_2 reagent streams merged together at the x confluence site, allowing the indicator reaction to proceed inside the following R_C coiled reactor. Baseline reflected then the own colours of the R_1 and R_2 reagents plus the degree of development of the non-catalysed indicator reaction. As the reaction occurred in the presence of iodide ions, the $[I_3]^-$ complex was formed and monitored at 420 nm [27]. The formation of this complex was dominant in the portions where the sample and R_1 volumetric fractions were optimized. Passage of the sample zone through the R_C reactor led to a transient increase in the rate of indicator reaction due to the analyte catalytic effects. During sample passage through

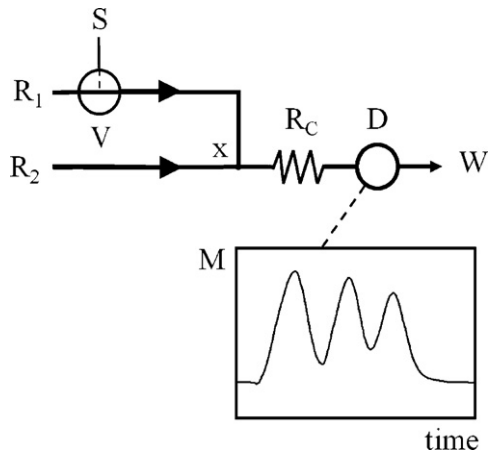

Fig. 1. Flow diagram. S = sample; R_1 = reagent carrier stream (0.1 mol L^{-1} KI in 0.01 mol L^{-1} HCl, 3.2 ml min^{-1}); R_2 = 0.001 mol L^{-1} Cr(VI), (0.6 ml min^{-1}); R_C = coiled reactor (200 cm); x = confluence point; V = solenoid valve; D = detector (420 nm); W = flask for waste collection; black arrows = sites where pumping is applied; empty arrow = flow direction; inset = typical recorder tracing (measurement M vs time function).

the detector, five different absorbance values (three maxima and two minima) were considered. Thereafter, the sample was discarded.

It should be stressed that R_1 stream is stopped for a short period of time during sample insertion. In this way, the R_1/R_2 volumetric ratio is modified along the dispersing zone, and this is another positive factor for selectivity improvement.

The influence of variations in sample volume (10–400 μL) and time interval between injections (10–18 s) were studied as shown in Table 1.

2.4. Data treatment

For building-up and calibrating the PLS models, 25 mixed standard solutions were used. Data were mean centred to remove any offset value and thereafter an internal leave-one-out cross validation procedure [29] was carried out. The number of PLS latent variables to be included in the model was selected by taking into account both the % captured variance and the root mean standard error prediction, RMSEP [30].

Table 1
Experimental design. S_i = sample injected volume (μL); Δt_i = time interval between insertions of plugs 1–2 and 2–3 (s). Data in parenthesis = volumes between plugs (μL), related to the Δt_i values.

Experiment number	S_1	S_2	S_3	Δt_1	Δt_2
1	400	300	200	13 (690)	10 (530)
2	300	200	100	13 (690)	10 (530)
3	200	100	80	13 (690)	10 (530)
4	100	80	50	13 (690)	10 (530)
5	80	50	30	13 (690)	10 (530)
6	50	30	10	13 (690)	10 (530)
7	400	300	200	15 (800)	13 (690)
8	300	200	100	15 (800)	13 (690)
9	200	100	80	15 (800)	13 (690)
10	100	80	50	15 (800)	13 (690)
11	80	50	30	15 (800)	13 (690)
12	50	30	10	15 (800)	13 (690)
13	400	300	200	18 (960)	15 (800)
14	300	200	100	18 (960)	15 (800)
15	200	100	80	18 (960)	15 (800)
16	100	80	50	18 (960)	15 (800)
17	80	50	30	18 (960)	15 (800)
18	50	30	10	18 (960)	15 (800)

For validation purposes, 16 randomly selected mixed standard solutions within 8.0–10.0 mg L^{-1} Fe and 6.0–8.0 mg L^{-1} V were used. The set of solutions for validation was different from that involved in the calibration step. Whenever required, the prediction ability of the model was evaluated.

3. Results and discussion

Formation of the tri-iodide complex initially dominated at the front, trailing edges of the dispersing sample plugs, as complete overlap of these coloured regions was not attained. After partial coalescence of the three inserted sample plugs, three overlapped peaks were recorded (Fig. 1) reflecting the concentration gradients established along the dispersing sample. Pronounced differences in maximal and minimal absorbance values were noted, emphasising the different catalytic effects of Fe(II) and V(IV) on the indicator reaction under different conditions. This aspect is fundamental for kinetic discrimination, thus for a proper modelling, as the measurements reflected the different fluid elements, reaction rates, timing and dispersion involved. With this strategy, measurements became less affected by variations in the flow system timing; hence the analytical procedure became potentially more rugged.

The effects of experimental variables such as sample volumes (S_1, S_2, S_3) and volumetric fraction of the reagents (Δt_1, Δt_2) on the determination of the both analytes were evaluated (Table 1). Selection of the experimental conditions relied on the estimated percentage of captured variance, number of latent variables, and RMSEP for iron and vanadium.

Good kinetic differentiation was always noted, as the influence of V(IV) on the rate of the indicator reaction was higher relatively to Fe(II). Sample volumes of 400, 300, 200 μL and Δt values of 18 and 15 s were selected. For smaller sample volumes and/or shorter time intervals, the prediction ability of the resulting models was impaired, as the time interval available for kinetic discrimination was not enough. On the other hand, for higher S_i and/or longer Δt_i values, complete separation of the sample plugs was noted and the main advantage of the proposal, namely exploitation of five potentially more precise measurements was lost.

Mathematical models involving different sample volumes (S_1, S_2 and S_3) and time intervals (Δt_1 and Δt_2) were built up, with the number of latent variables ranging between LV_1 and LV_5. Analysis of Fig. 2 revealed that a good compromise between model predictive capacity and number of latent variables was attained by using sample volumes of 400, 300, 200 μL and Δt values of 18 and 15 s. In this situation, corresponding to the experiment #13 specified

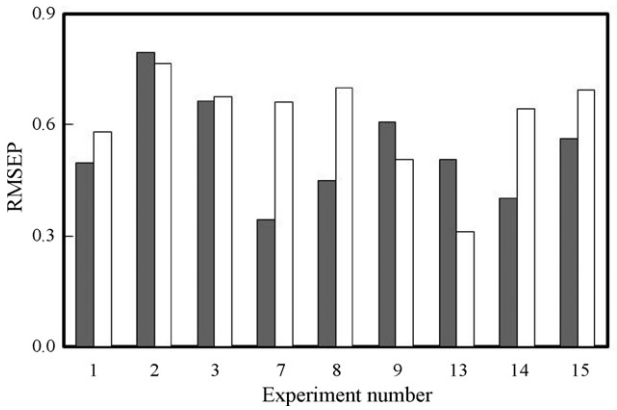

Fig. 2. Root mean standard error predictions. RMSEP values for iron (gray bars) and vanadium (empty bars) refer to the experimental conditions in Table 1, and are expressed in %.

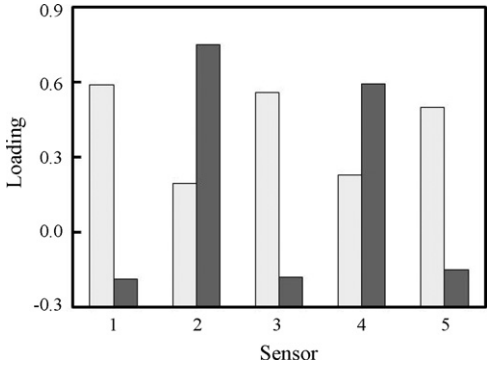

Fig. 3. Loading plot. Figure refers to the LV_1 (empty bars) and LV_2 (gray bars) latent variables. Sensor refers to the slice of the sample zone associated to the maximal and minimal absorbance values. As each measurement is characterized by specific concentrations and timing, one can imagine that there is a pseudosensor adherent to it.

Table 2
Comparative results. Data in % (w/w). Iron and vanadium concentrations in Fe/V alloys determined by the proposed procedure (FIA) and by ICP-OES (uncertainties typically 2%). Uncertainties based on four replicated analysis.

Sample	Fe		V	
	FIA	ICP-OES	FIA	ICP-OES
1	48.1 ± 0.1	47.6	35.1 ± 0.1	33.8
2	42.8 ± 0.2	43.5	34.1 ± 0.2	34.8
3	46.7 ± 0.1	45.5	37.7 ± 0.2	36.6
4	48.9 ± 0.2	49.6	38.7 ± 0.4	38.3

in Table 1, *ca* 95% of total variance inherent to the data set were captured by the two first two latent variables. Number of latent variables was then selected as 2.

Regarding the loading plot (Fig. 3), one can perceive that first latent variable reflects the regions of the sample zone characterized by maximal and minimal absorbance values. The differences between loading values related to LV_1 and LV_2 are then due to the differences in catalytic effects of the involved ions. In fact, the influence of V(IV) in the indicator reaction rate is more significant relatively to Fe(II).

The proposed system is simple and rugged, and no baseline shift was noted after extended (4 h) working periods. About 25 samples are run per hour, meaning 50 determinations. Consequently 60 mg KI and 0.11 mg Cr(VI) are consumed per determination. After ten replications of a typical sample, standard deviations of measurements were estimated as around 0.008 absorbance (1.6%). As expected, these values were better relatively to those associated to the gradient regions of the dispersed sample, for which higher values were always noted.

Accuracy was assessed by comparing the results with those obtained by inductively coupled argon plasma optical emission spectrometry [31] (Table 2). Application of the paired *t*-test revealed that there is no difference between methods at the 95% confidence level (t) values: 0.049 (Fe) and 0.159 (V); critical limit = 3.18). Relative standard deviations of results were estimated as 1.9% and 2.7% for Fe and V, respectively. It is interesting to report that, less precise measurements were noted for some samples from time to time. Hopefully, these adverse effects did not influence the final results in a pronounced way, as the model relied on a large dataset.

4. Conclusions

The feasibility of this strategy for implementing differential kinetic analysis in a flow system was demonstrated and excellent analytical figures of merit were attained. Parallel experiments revealed that the proposed system can be applied for Fe, V and Ti determinations, as Ti(IV) also influences the indicator reaction rate. No additional analytical steps would be required. This result opens the possibility of designing analogous flow systems for multiparametric analyses exploiting differences in reaction rates.

For sample batches with low variability in the analyte concentrations such as those used in the present work, preparation of mixed working standards covering narrower concentration ranges restricts the model to these ranges, and this feature is an additional guaranty for analytical accuracy.

Acknowledgements

The authors thank FAPESP (processes 06/03859-9 and 2006/07309-3) for financial support and CAPES/GRICES (proc. 197/06) for the fellowships.

References

[1] J.H. Dahl, D. Espersen, A. Jensen, Anal. Chim. Acta 105 (1979) 327–333.
[2] D. Espersen, A. Jensen, Anal. Chim. Acta 108 (1979) 241–247.
[3] H. Kagenow, A. Jensen, Anal. Chim. Acta 114 (1980) 227–234.
[4] J. Ruzicka, J.W.B. Stewart, E.A.G. Zagatto, Anal. Chim. Acta 81 (1976) 387–398.
[5] A. Fernandez, M.A. Gomes-Nieto, M.D. Luque de Castro, M. Valcarcel, Anal. Chim. Acta 165 (1984) 217–226.
[6] F. Lazaro, M.D. Luque de Castro, M. Valcarcel, Anal. Chim. Acta 169 (1985) 141–148.
[7] P. Linares, M.D. Luque de Castro, M. Valcarcel, Talanta 33 (1986) 889–893.
[8] P. Linares, M.D. Luque de Castro, M. Valcarcel, Microchem. J. 35 (1987) 120–124.
[9] C.C. Oliveira, R.P. Sartini, B.F. Reis, E.A.G. Zagatto, Anal. Chim. Acta 332 (1996) 173–178.
[10] H. Muller, V. Muller, E.H. Hansen, Anal. Chim. Acta 230 (1990) 113–123.
[11] R. Kuroda, T. Nara, K. Oguma, Analyst 113 (1988) 1557–1560.
[12] E.A.G. Zagatto, H. Bergamin-Filho, S.M.B. Brienza, M.A.Z. Arruda, A.R.A. Nogueira, J.L.F.C. Lima, Anal. Chim. Acta 261 (1992) 59–65.
[13] D. Vendramini, V. Grassi, E.A.G. Zagatto, Anal. Chim. Acta 570 (2006) 124–128.
[14] X.-J. Peng, Q.-K. Mao, J.-K. Cheng, Fresenius J. Anal. Chem. 348 (1994) 644–647.
[15] P. Richter, M.I. Toral, A.E. Tapia, C. Ubilla, M. Bunster, Bol. Soc. Chil. Quim. 41 (1996) 167–172.
[16] A. Espinosa-Mansilla, F. Salinas, A. Zamora, Mikrochim. Acta 113 (1994) 9–17.
[17] M.A.Z. Arruda, E.A.G. Zagatto, N. Maniasso, Anal. Chim. Acta 283 (1993) 476–480.
[18] A. Fernandez, M.D. Luque de Castro, M. Valcarcel, Anal. Chem. 56 (1984) 1146–1151.
[19] M. Agudo, J. Marcos, A. Rios, M. Valcarcel, Anal. Chim. Acta 239 (1990) 211–220.
[20] J.F. Tyson, Analyst 112 (1987) 523–526.
[21] D.A. Whitman, M.B. Seasholtz, G.D. Christian, J. Ruzicka, B.R. Kowalski, Anal. Chem. 63 (1991) 775–781.
[22] P.R. Fortes, S.R.P. Meneses, E.A.G. Zagatto, Anal. Chim. Acta 572 (2006) 316–320.
[23] J. Saurina, S. Hernandez-Cassou, Anal. Chim. Acta 438 (2001) 335–352.
[24] E.A.G. Zagatto, M.F. Gine, E.A.N. Fernandes, B.F. Reis, F.J. Krug, Anal. Chim. Acta 173 (1985) 289–297.
[25] R.A.S. Lapa, J.L.F.C. Lima, B.F. Reis, J.L.M. Santos, E.A.G. Zagatto, Anal. Chim. Acta 466 (2002) 125–132.
[26] Annual Book of ASTM International Standards 2008, Section 3, Metals Test Methods and Analytical Procedures, Analytical Chemistry for Metals, Ores and Related Materials (I): E32-latest, vol. 3.05, 2008.
[27] J. Wang, R. He, Anal. Chim. Acta 276 (1993) 419–424.
[28] M.A. Feres, P.R. Fortes, E.A.G. Zagatto, J.L.M. Santos, J.L.F.C. Lima, Anal. Chim. Acta 618 (2008) 1–17.
[29] D.M. Haaland, E.V. Thomas, Anal. Chem. 60 (1988) 1193–1202.
[30] D.L. Massart, B.G.M. Vandeginste, S.N. Deming, Y. Michote, L. Kaufman, Chemometrics: A Textbook, Elsevier, Amsterdam, 1988.
[31] A.O. Jacintho, B.R. Figueiredo, B.F.Reis, E.A.G. Zagatto, F.J. Krug, M.F. Gine, M.C.U. Araujo, N.M. Pereira, R.E. Bruns, Análise Química de Rochas por ICP-AES, Ed. Unicamp, Campinas, Brazil, 1985.